

Evaluation of Gas Turbines as alternative energy production systems for a large cruise ship to meet new maritime regulations

A. Armellini*, S. Daniotti*, P. Pinamonti*, M. Reini°

**Polytechnic Department of Engineering and Architecture, University of Udine, via delle Scienze, 208, 33100 Udine (UD), Italy*

°Department of Engineering and Architecture, University of Trieste, via Valerio, 10, 34128 Trieste (TS), Italy

Abstract

As a consequence of the new and up-coming regulations imposed by the International Maritime Organization (IMO), polluting emissions produced by large ships are now under strict control. Moreover, specific areas called “Emission Controlled Area” (ECA), which request even lower pollutant emissions, will be extended.

To face up to this issue, ships propelled by Internal Combustion Engines (ICEs) burning Heavy Fuel Oil (HFO) can be equipped with abatement devices such as scrubbers and Selective Catalytic Reactor systems. Along with these solutions, which seem to be the route ship-owners will prefer, other methods can be considered, such as the use of Marine Gas Oil (MGO): a more expensive fuel, but with lower sulphur content. The use of MGO allows users to consider a further and more drastic modification of the power system, namely the use of Gas Turbines (GTs) in place of ICEs. GTs, despite being less efficient, are much lighter, more compact, and can more easily reach low NO_x emissions than ICEs. Even if these aspects are theoretically well known, there are still difficulties in finding studies reporting quantitative analysis (weight, dimensions, fuel consumption) that compare GT and ICE power systems employed on board.

The present paper aims to provide these data by analyzing different solutions applied to a real case. Unlike other studies, the work is focused on a cruise ship rather than on a cargo ship, because a cruise ship’s operation profile is more variable during the trip.

Keywords: IMO, Cruise ship, Emissions, Optimization, Gas Turbines

Nomenclature

%MCR	Maximum Continuous Rating	[%]
DWT	Dead Weight Tonnage	[ton]
EEDI	Energy Efficiency Design Index	[$\text{gCO}_2/\text{ton/miles}$]
E_{cl}	global electric load	[kJ]
EF_h	h-th pollutants Emission factor	[$\text{g}_{h\text{-th,pollutants}}/\text{kg}_{\text{fuel}}$]
$EF_{ICE_NO_x}$	ICE’s NO_x emission factor	[$\text{g}_{\text{NO}_x}/\text{kg}_{\text{fuel}}$]
$EF_{ICE_SO_x}$	ICE’s SO_x emission factor	[$\text{g}_{\text{SO}_x}/\text{kg}_{\text{fuel}}$]
E_{fuel}	Single cruise time interval fuel energy	[kJ]
$E_{\text{fuel,big,ICEs}}$	Single cruise time interval fuel energy for “big” internal combustion engines	[kJ]
$E_{\text{fuel,OFBs}}$	Single cruise time interval fuel energy for Oil Fired Boilers	[kJ]
$E_{\text{fuel,PMs}}$	Single cruise time interval fuel energy for Prime Movers	[kJ]
$E_{\text{fuel,small,ICEs}}$	Single cruise time interval fuel energy for “small” internal combustion engines	[kJ]
$E_{\text{fuel,global}} (=FE)$	Global cruise fuel energy	[kJ]
$E_{\text{fuel,global_OFBs}}$	Global cruise fuel energy for Oil Fired Boilers	[kJ]
$E_{\text{fuel,global_PMs}}$	Global cruise fuel energy for Prime Movers	[kJ]
EL	Total electric loads	[kW]
$EL_{\text{prop.}}$	Propulsive electric loads	[kW]
$E_{TH,ACC.}$	Ship global accommodation thermal load	[kJ]
$E_{TH,ACC.-EGBs}$	Accommodation thermal loads recovered in Exhaust gas boilers	[kJ]
$E_{TH,ACC.-OFBs}$	Accommodation thermal loads supplied by Oil Fired Boilers	[kJ]

$E_{TH,FW}$	Ship global thermal load for fresh water production	[kJ]
$E_{TH,FW,-Cogen}$	Fresh water production thermal load covered by cogeneration	[kJ]
$E_{TH,FW,-OFBs}$	Fresh water production thermal load covered by Oil Fired Boilers	[kJ]
FE	Fuel energy content	[kJ]
Fuel	Fuel burned	[ton]
h	h-th pollutants	
k	Single cruise time interval	
LHV	Lower Heating Values	[kJ/kg]
n _{pep}	Non-propulsive electric loads	[kW]
PE _h	h-th pollutants emissions	[ton]
t	Integer Number of ICE type "small" operating in the k-th cruise time interval (0, 1 or 2)	
T _{g OUT EGB}	Exhaust gas temperature of EGB	[°C]
TIT	GT Turbine Inlet Temperature	[°C]
TOT	GT Turbine Outlet Temperature	[°C]
u	Integer Number of ICE type "big" operating in the k-th cruise time interval (0, 1 or 2)	
η	Efficiency	
η_{OFB}	Oil Fired Burners efficiency	
η_{SCR}	Selective Catalytic Reactor efficiency	
$\eta_{scrubber}$	Scrubber efficiency	
$\eta_{ship,global}$	Global ship's energy efficiency	

Acronyms

A	Autumn
ACC	Accommodation
COP	Coefficient of Performance
ECA	Emission Controlled Area
EGBs	Exhaust Gas Boilers
ER	Engine Room
FW	Fresh Water
GHG	Green House Gas
GT	Gas Turbine
HFO	Heavy Fuel Oil
ICE	Internal Combustion Engine
ICE _{eco}	Internal Combustion Engine in “ecofriendly” mode with SCR and scrubber installed on board
IMO	International Maritime Organization
LNG	Liquefied Natural Gas
MARPOL	Maritime Pollution policies
MGO	Marine Gas Oil
MINLP	Mixed Integer Non Linear Programming
MSF	Multi Stage Flash evaporator
MVDC	Medium Voltage Direct Current
OFBs	Oil Fired Burners
ORC	Organic Rankine Cycle
PMs	Prime Movers
RPM	Rated Engine Speed
S	Summer
SCR	Selective Catalytic Reactor
SECA	SO _x Environmental Controlled Area
SEEMP	Ship Energy Efficiency Management Plan
TH	Tanks Heating
W	Winter

1. Introduction

The Maritime Transport sector consists of a heterogeneous group of vessels, which can be divided into two major classes: “goods transport” and “passenger transport”. The first class accounts for 90% of the overall worldwide transportation, [1] but the second has doubled its market in the last decade [2]. Vessel engines have to burn fossil fuels to conduct their activities, causing both Green House Gases (GHGs) and non-GHG emissions. The former are responsible for climate change; the latter for acid rain, the decrease of agricultural yields, water contamination, modification of soil biology, deforestation and for damaging monuments. Emissions trading, financial incentives, emission monitoring obligations, and emissions (or energy efficiency) standards are the most used regulation mechanisms to reduce the environmental impact connected to the shipping industry. The most noteworthy regulator in the shipping industry is a specific branch of the United Nations, namely International Maritime Organization (IMO), which, in 2013, introduced two new policy mechanisms aiming to cut down GHG emissions: the Energy Efficiency Design Index (*EEDI*) and the Ship Energy Efficiency Management Plan (SEEMP). According to Anderson and Bows [3], the target of keeping the global temperature increase below 2°C, compared to preindustrial level will imply a reduction of carbon emissions from shipping by more than 80% compared to 2010 levels.

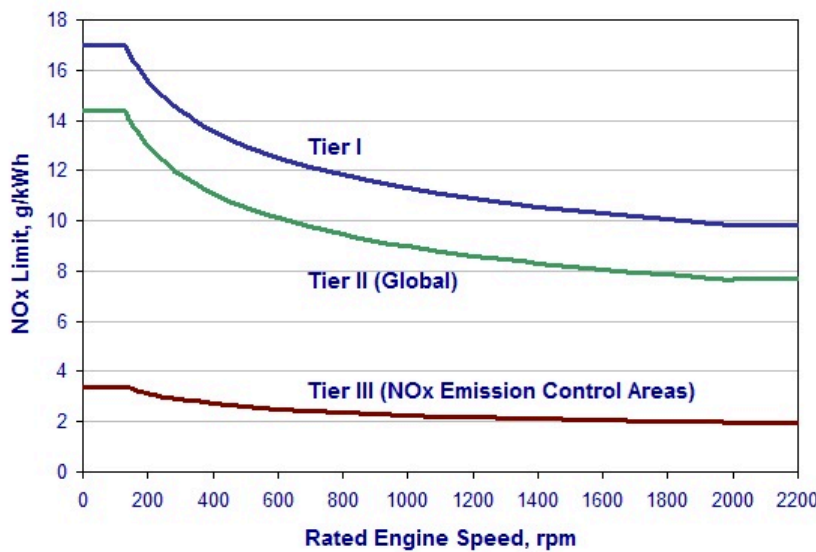


Fig. 1. MARPOL NO_x's threshold limits values [6].

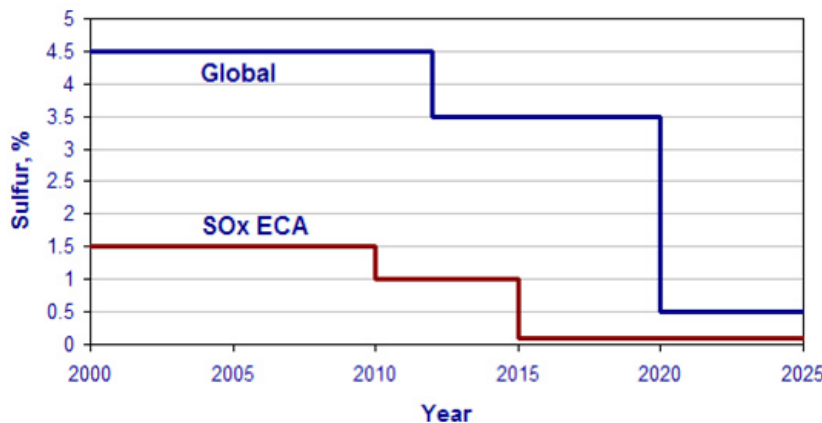


Fig. 2. MARPOL SO_x threshold limits values [6].

IMO regulates non-GHG emissions too. The most prominent convention, the International Convention for the Prevention of Ship's Pollution (MARPOL), was adopted in 1973 and it targeted several aspects of air pollution. “Annex VI,” which was added to the convention in 1997, addresses exhaust gas emissions such as SO_x, NO_x, and particulates [4]. Since NO_x and SO_x emissions have been increasing in these years [5], IMO is setting a lower threshold values.

Particular attention has been given to SO_x Emission Controlled Areas (SECAs), regarded as needing an immediate intervention.

MARPOL addresses NO_x pollutants with three “tiers”: each tier consisting of a description of limits imposed on ships in relation to ICE engine RPM, as can be seen in Fig. 1. Nowadays only ships travelling in the Emission Controlled Areas (ECAs) have to observe emission limits of Tier III, but starting from January 1st 2016 every ship has to [6].

Regarding SO_x emissions, MARPOL currently sets limits on the fuel sulphur content, differentiating from SECA and not-SECA areas. From 2015, ships travelling in the SECA seas had to use fuel with less than 0.1% sulphur content. Outside SECA areas the limit imposed is set at 3.5%, but starting from 2020 also non-SECA areas will be subjected to a drastic reduction of the sulphur threshold value of the fuel employed at 0.5% (Fig. 2) [6].

As a consequence of the cited limits and regulations, ship-owners will have to adopt new strategies and solutions in order to be IMO compliant. In order to respect *EEDI* and *SEEMP*, ships have to be more efficient in terms of fuel consumption. Along with ship efficiency improvement, other interventions have been made to meet with the new and stricter non-GHG emissions limits.

Using low-sulphur fuel is the easiest way to overcome the SO_x issue. Despite being the easiest method, switching kind of fuel could be very expensive and other solutions could be more feasible.

In 2012, Lloyd’s Register carried out a survey asking 14 of the world’s leading shipping companies about their intention on implementing technologies to mitigate SO_x emissions in order to meet the new regulations [7]. It emerged that employing low-sulphur distillate, for instance MGO, is currently considered the best short-term solution for SO_x mitigation, with a DeSO_x system called *scrubbers* being better in the medium term, and dual-fuel/ LNG preferred for the longer-term [7], as can be inferred from Figure 3. LNG is presently established as a clean and reliable fuel for ship propulsion and auxiliary on board power generation [8, 9, 10] but it has still problems concerning safety (high flammability and toxicity [11]) as well as lack of infrastructures. Hence, two alternatives are at hand to cut down SO_x emissions: either equipping ships with scrubbers or replacing the currently used fuel with a sulphur-free one, for instance MGO.

NO_x emissions can be reduced in various ways [12, 13] but, contrary to what happens for SO_x emissions, switching type of fuel would not prevent ships from having to install a specific abatement device, even if there is an ongoing evolution of combustion systems of diesel engines. Selective Catalytic Reactor (SCR) systems are the most frequently used, thanks to their higher capability to cut down ship NO_x emissions, compared to other abatement devices, as is reported in Figure 4 [14]. Very recently, Exhaust Gas Recirculation (EGR) applications for large marine Diesel engine have claimed NO_x reduction potential up to 90%, for both 2 stroke [15] and 4 stroke [16] engines.

Abatement devices, like De-SO_x and De-NO_x, along with their auxiliaries, occupy space and increase the overall weight of the ship, as well as worsen the fuel consumption due to the bigger electric load. An increase of weight and volume is also implied by the adoption of some additional thermal cycle, bottoming ICE, like Organic Rankine Cycle (ORC) [17-21], Brayton [22], Brayton + Rankine [23]. These solutions aim to improve the electrical efficiency of the propulsion system and therefore, to reduce the overall emission levels.

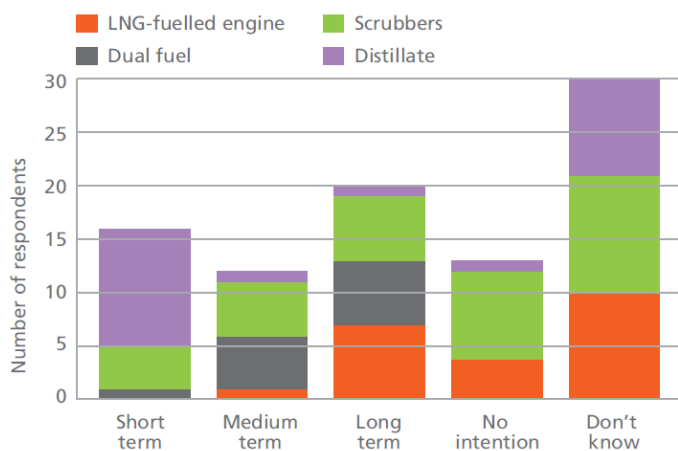


Fig. 3. Shipowners’ survey – intentions for mitigating SO_x emissions [7].

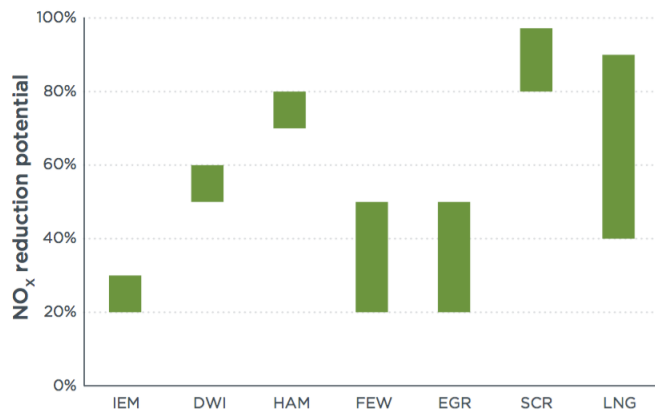


Fig. 4. Shipping NO_x reduction potential. IEM: Internal Engine Modification, DWI: Direct Water Injection, HAM: Humid Air Motors, FEW: Fuel Water Emulsion, EGR: Exhaust Gas Recirculation, SCR: Selective Catalytic Reduction, LNG: Liquefied Natural Gas [14].

Since saving space and weight is a big issue in the maritime sector, a completely different solution could be taken into consideration, namely the use of MGO to get SO_x free emissions and the consequent use of GTs in place of ICEs. This drastic modification of the power generation system aims to reduce weight and increase space, obtaining a dramatic reduction of pollutant emissions level, compliant with the IMO regulations, and keeping a good efficiency level [24]. Moreover, due to the high rotational speed usually characterizing GT operation, the coupled generators are not as big as those of ICEs, meaning a further reduction in weight and occupied space. Finally, as shown in a recent industrial research project [25], these power generation and conversion systems are well coupled with a power grid working in Medium Voltage Direct Current (MVDC).

As can be easily foreseen, the drawback of this solution is the negative gap that is found in the energy conversion efficiency of GTs opposed to that of ICEs, and in the higher cost of MGO than the cheaper HFO.

In order to evaluate the technical and economic feasibility of this solution, it is essential to be able to quantify the positive aspects coming from room and weight savings against the effective increase of fuel consumption. This evaluation is not trivial, since a ship is a closed and complex energy system, whose operation profile might be extremely variable, and where energy recovery strategies are always implemented in order to reduce the waste heat by partial cogeneration of the thermal loads. With particular regard to the latter aspect, it is also important to consider that, thanks to the high temperature of GTs exhaust gas flows, a higher energy recovery can be achieved, hence reducing the initial efficiency gap between GTs and ICEs intended as Prime Movers (PMs).

Until now, few studies can be found in literature about the adoption of GTs as PMs in cruise ships. One example of an existing cruise ship adopting gas turbines is the “Millennium”, launched in the year 2000. The Millennium has a power plant consisting in a combined cycle of two 25MW “LM2500+” gas turbines burning MGO, bottomed by a 9 MW steam turbine, which is powered by the GT’s exhaust flows heat [26, 27]. This solution allows high efficiency and low **pollutant emissions compared with conventional ICE, but also operation and investment costs are expected to be much higher**, therefore no other cruise ship with this propulsion solution has been designed.

Dealing with the design of land based systems for the energy production and process industry sectors, a lot of feasible engine configurations as well as waste heat recovery options have been considered in literature, often with the help of some optimization procedures (see, for instance, [28-35]), but only few studies can be found in literature for marine energy systems [36, 37].

The present work aims at evaluating different possible engine configurations, which can be adopted on board a large cruise ship, in order to get the best compromise-solutions for environmental pollution, energy consumption and space occupation (weights & volumes). All these points of view are extremely important for the maritime sector, in particular for cruise ships, because they are particularly energy consuming and because the energy needs they have to satisfy are much more irregular than the ones of Cargo Ships. Cruise liners have a passenger capacity of a few thousand persons with a crew of several hundreds. The principal energy demands of such vessels are propulsion power, electricity for covering the hotel related loads and heat in the form of water, or low pressure steam, for heat driven auxiliary equipment and sanitary purposes. A preliminary investigation has been presented in [38].

In this study, in particular, the on board energy system of a large cruise ship has been analyzed and optimized by using operating data coming from a real case. The conventional solution actually implemented (ICE fed with HFO) is then compared with two alternative solutions: ICE fed with HFO and equipped with De-NO_x / De-SO_x devices (ICE_{eco}) and GT fed by MGO.

Studies reporting quantitative analysis (weight, dimensions, fuel consumption) that compare GT and ICE power systems employed on board are still not common in literature. The present paper aims to provide these data by analyzing different solutions, considering not only the engine design operating conditions, but the actual expected conditions during a typical cruise. The results can be a starting point for the economical evaluation of the different technologies by the ship owners, taking into account fuel costs, emission abatement requirements and profitable space availability.

2. Case study

A real cruise ship operation profile has been used as the case study. The reference cruise ship is the hull C.6194 of Fincantieri S.p.A. having 66000 Dead Weight Tonnage (DWT). An Integrated Power System based on a diesel-electric propulsion system characterizes this project. The hull under examination is used in a tourist cruise between Barcelona and Venice. Fincantieri S.p.A. has supplied the documentation reporting the design operation profile within a research project in which the Department of Electrical, Mechanical and Management Engineering of the University of Udine collaborated as a partner [25].

The reference cruise consists of 50 time intervals divided in 3 phases: harbor, maneuvering and navigation. A preliminary analysis of the operation profile has showed that harbor and navigation phases are the more time-consuming, accounting for 46% and 47% of the whole cruise respectively. Specific electric demands (propulsive and non-propulsive loads) as well as particular thermal loads characterize each time interval. Thermal loads and non-propulsive electric loads have also seasonal variations as a consequence of the different location, the sea and the ship's internal air temperatures.

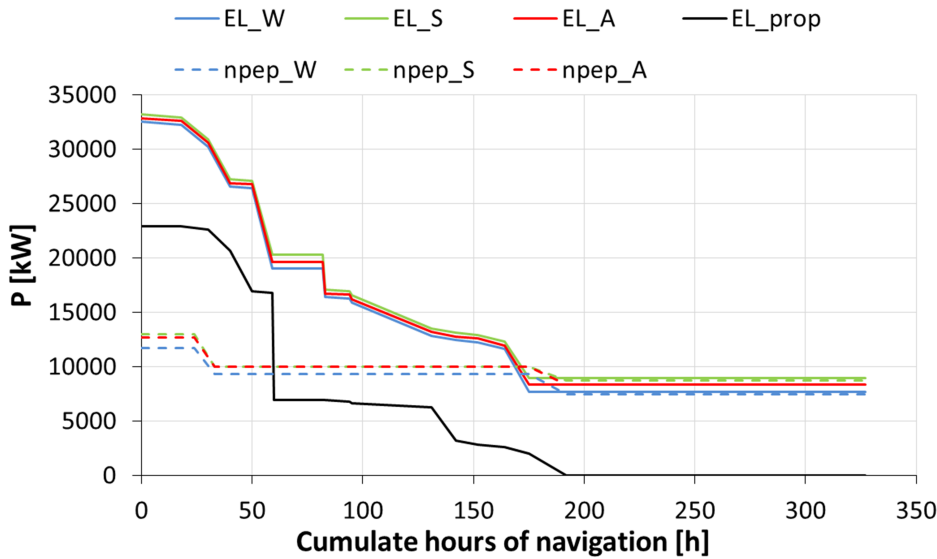


Fig. 5. Variations of the electric power demands on cruise at different seasons. Data obtained from [39].

Figure 5 represents the variation of the total electric loads (EL), divided into propulsive electric loads (EL_{prop}) (bold black line) and non-propulsive electric loads ($npep$) (dashed colored lines), during the cruise for the typical seasons of the year, Winter (W), Summer (S) and Autumn (A), where the loads in Autumn are regarded as similar to Spring ones in the whole year computation. The chilling electric loads have been considered as well; they are counted within the non-propulsive electric loads and they vary from a minimum of 0.3 MW to a maximum of 2.2 MW occurring in winter-harbor condition and in summer-navigation, respectively. These loads are produced by four 800 kW compressors, whose Coefficient Of Performance (COP) is equal to 4.9, to cover the chilling loads [39].

The analysis of the operation profile also showed the existence of a “base load” condition that occurs for 42% of the whole cruise but that also represents the minimum working load (namely about one fourth of the peak load). This operational condition is clearly quite demanding. In order to overcome this issue and to obtain the highest energy conversion efficiency possible, the total power installed on board the reference ship has been divided among 4 engines

(2 “small” and 2 “big”, as will be reported in System model). This solution allows acting primarily on the number of active engines and only successively on the load modulation of each engine.

The thermal loads are divided into three macro-poles: Tanks Heating (TH), Engine Room (ER) (both of them connected to the fuel handling and lubricants devices), and Accommodation (ACC), i.e. the thermal loads deriving from “hotel” services. Along with these thermal loads, there is another thermal load, which requires lower temperatures to be satisfied, namely the Fresh Water (FW) production, provided by the use of two Multi Stage Flash (MSF) generators, having a capacity of 50 t/day and a consumption of 0.144 kWh/kg_{FW} [40].

Because of the different temperature levels that are required by the various thermal loads, their coverage is satisfied with multiple sources, namely: steam flow at 182°C and 11.5 bar produced by the Exhaust Gas Boilers (EGBs) operated with the engines exhaust gas flows, and hot water deriving from the high temperature engines cooling circuit. Therefore, cogeneration is already employed on the reference cruise ship. When the aforementioned cogeneration sources cannot satisfy the thermal loads, Oil Fuel Burners (OFBs) are used as backup solutions. The ship examined in this study has two OFBs producing steam at a capacity of 10 t/h, burning HFO with an efficiency of 90% [39].

3. Methodology

In the present work, the reference on board energy system of the cruise ship has been modeled as depicted in Figure 6. In more detail, depending on the kind of PMs considered, internal combustion engines or gas turbines, it is possible to have two engine configurations: ICE and GT. Within the ICE configuration, the employment of SCRs and scrubbers results in a further configuration, called ICE_{eco}. Therefore, three engine configurations, namely ICE, ICE_{eco} and GT are considered. Models of PMs, EGB as well as the exhaust gas after treatment devices are reported in the following paragraph (System model).

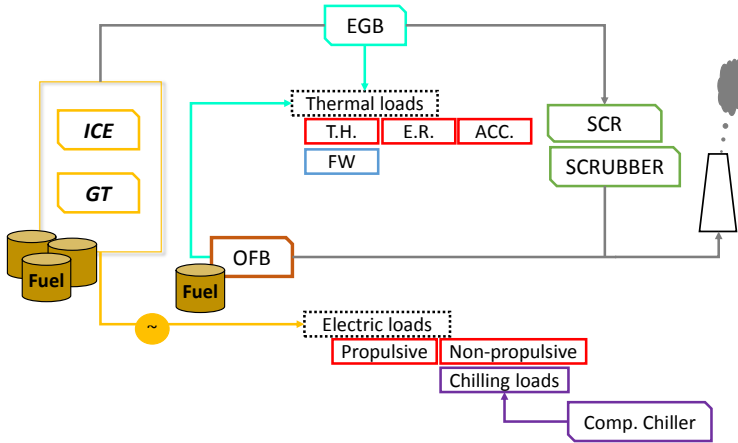


Fig. 6. Reference model of the cruise ship's energy system.

Because of the constraints imposed by the specific application under exam, the number of possible options regarding the components designs and synthesis is restricted to some kind of engines sizes and technologies. Thus, these options have been kept external to the optimization procedure, whose target is to find the system's optimal operation profile. Since there are both discrete and continuous variables as well as non-linear functions, the problem under examination falls under the general category of Mixed Integer Non Linear Programming (MINLP), which combines the combinatorial difficulty of optimizing over discrete variable sets with the challenges of handling nonlinear functions. From a literary review, it has been chosen to follow the same method used by Dimopoulos et al. in [41], which is a heuristic one.

The aim of the optimization carried out in the present work is to ensure that the highest global ship energy efficiency, expressed by means of Eq. (1), is achieved within the simulated operation profiles:

$$\eta_{ship,global} = \frac{E_{el.} + E_{TH,ACC.} + E_{TH,FW}}{E_{fuel,global}} \quad (1)$$

where $E_{el.}$ is the ship's global electric load (consisting of propulsive and accommodation electric loads), $E_{TH,ACC.}$ is the ship's global accommodation thermal load, $E_{TH,FW.}$ is the ship's global thermal load for fresh water production, $E_{fuel,global}$ is the global energy content of the burned fuel both in the prime movers and in the OFBs.

Thermal loads linked to TH and ER users have not been taken into account in the efficiency definition, because only those effects allowing the ship to move and provide facilities to the customers have been considered.

On the other hand, the denominator represents the overall amount of fuel burnt in PMs, and hence also that amount used to satisfy the TH and ER users thermal loads.

Analyzing Eq. (1), the only way to enhance the ship energy efficiency is by lowering the overall amount of $E_{fuel,global}$, determined by Eq. (2):

$$E_{fuel,global} = E_{fuel,global_PMs} + E_{fuel,global_OFBs} \quad [kJ] \quad (2)$$

where the terms expressing the amount of fuel globally burned in PMs ($E_{fuel,global_PMs}$) and in OFBs ($E_{fuel,global_OFBs}$), are given by Eq. (3) and Eq.(4), respectively:

$$E_{fuel,global_PMs} = \sum_{k=1}^{50} E_{fuel_PMs_k} \quad [kJ] \quad (3)$$

$$E_{fuel,global_OFBs} = \sum_{k=1}^{50} E_{fuel_OFBs_k} \quad [kJ] \quad (4)$$

where the index k represents the k -th cruise time interval.

Since OFBs work to satisfy thermal loads, $E_{fuel,global_OFBs}$ burned by them depends on how much waste heat from PMs' exhaust gas is exploited to cover thermal loads, i.e. the percentage of cogeneration, as determined in Eq. (5):

$$Cogeneration \% = 1 - \frac{E_{TH,ACC.-OFBs} \times \eta_{OFB} + E_{TH,FW.-OFBs} \times \eta_{OFB}}{E_{TH,ACC.} + E_{TH,FW}} \quad (5)$$

where $E_{TH,ACC.-OFBs}$ is the accommodation thermal load covered by OFB use, $E_{TH,FW.-OFBs}$ is the thermal load for the fresh water production satisfied by OFBs, η_{OFB} is OFB thermal efficiency.

Thermal loads satisfied by OFBs are determined by Eq. (6) and (7) concerning accommodation thermal loads and fresh water production thermal loads respectively:

$$E_{TH,ACC.-OFB} = E_{TH,ACC.} - E_{TH,ACC.-EGBs} \quad [kJ] \quad (6)$$

$$E_{TH,FW.-OFB} = E_{TH,FW.} - E_{TH,FW.-Cogen.} \quad [kJ] \quad (7)$$

where $E_{TH,ACC.-EGBs}$ is the accommodation thermal load covered by the exhaust gas waste heat recovery through EGBs, $E_{TH,FW.-Cogen.}$ is the thermal load for the fresh water production.

Thermal load for the FW production is fulfilled in two different ways, depending on PM typology:

- ICE: exploitation of engines cooling water high temperature circuit;
- GT: exploitation of the remaining exhaust gas waste heat content having satisfied the accommodation thermal load.

Generally, heat recovered by exhaust gas exploitation is proportional to exhaust gas mass flow and temperature, which mainly depend on a single factor: $\%MCR$, for both kinds of prime movers. In consequence of the present strong use of cogeneration, to find the optimal $\%MCR$ that realizes the minimum $E_{fuel,global}$ for each cruise time interval is not trivial. Indeed, the need to rigidly satisfy at the same time both electrical and thermal loads implies that for each case the best percentage of cogeneration must be sought, i.e. a compromise between exhaust gas waste heat exploitation and OFB use is necessary. Therefore, the optimization procedure has to identify the operation that leads to determine the maximum ship energy efficiency for each cruise time interval (or equivalently the minimum E_{fuel} burned), characterized by the specific electric and thermal loads.

Consequently, the optimization task that has been accomplished for each configuration, each k -th cruise time interval, and each season is stated by Eq. (8) with the constraints expressed by Eq. (9):

$$\text{minimize } E_{fuel} = t \times E_{fuel,small,ICE} + u \times E_{fuel,big,ICE} + E_{fuel,OFBs} \quad (8)$$

$$0 \leq t, u \leq 2$$

$$0.5 \leq \%MCR \leq 1 \quad (9)$$

Where t , u represent the number of active small and big engines, respectively, $E_{fuel,small,ICE}$ and $E_{fuel,big,ICE}$ are the amounts of fuel burned in the smallest and biggest ICE respectively, and $E_{fuel,OFBs}$ is the amount of fuel burned in the OFBs. Eq. (8) and (9) apply also for GT configuration. For each k-th cruise time interval, the Evolutionary Algorithm has to decide which engine to switch on.

The constraint of 0.5 imposed to the minimum allowable $\%MCR$, has been set in order to limit the possible number of solutions that have to be investigated, hence excluding those characterized by too high fuel consumption and pollutant emissions. Furthermore, the value of $E_{fuel,global}$ is given in terms of energy-fuel content instead of tons of fuel to overcome the issue coming from handling fuels having different Lower Heating Value (LHV).

The thermal and electrical demands are additional constraints, which have to be satisfied in each time interval of the cruise. Further constraints have been introduced in the optimization statement, concerning the models of PMs and EGBs, which are described in the next paragraphs. In particular, the general function expressed by Eq. (10) represents that of PMs, which can be applied also to EGBs, once having substituted the amount of energy-fuel burnt with the thermal power recovered through the exhaust gas exploitation:

$$E_{fuel,PMs} = f(\%MCR_{PMs}) \quad (10)$$

To optimize $E_{fuel,global}$, a single objective optimization procedure has been implemented in Microsoft Excel® and, along with energy efficiency, pollutants emissions are finally calculated. In the present work five kinds of pollutant emissions are considered: NO_x , SO_x , CO, PM and HC.

4. System model

The present section describes the numerical models that have been used to simulate the operation of the various components involved in the ship scheme reported in Figure 6.

An analysis of these three kind of solutions (ICE, ICE_eco and GT) has been carried out to extrapolate the trade-off between engine efficiency and loads, the quality and quantity of the waste heat recoverable through EGB as well as engine weight and volume.

4.1 Internal Combustion Engines

In the reference cruise ship, 4-stroke-turbocharged-intercooled diesel engines are employed, namely two “big” ones of about 12.6 MW (Wärtsilä W12V46C), and two “small” ones of about 8.4 MW (Wärtsilä W8L46C).

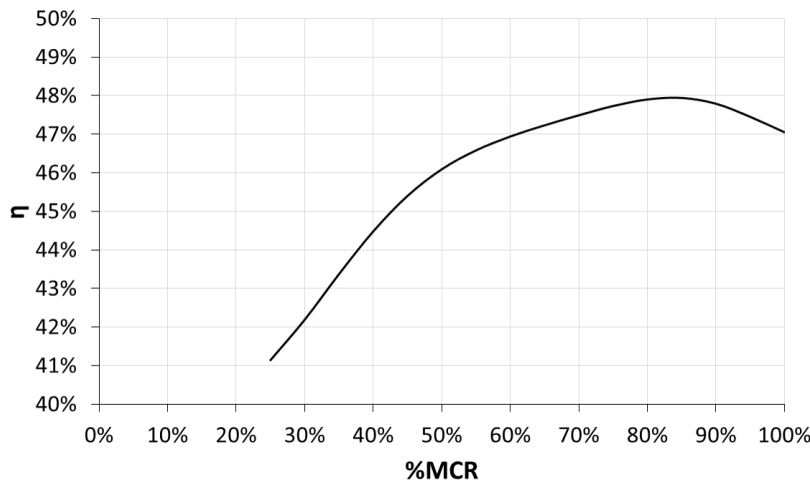


Fig. 7. Behavior of the engine efficiency vs. load % for the Wärtsilä #46C internal combustion engine, at fixed RPM. Data obtained from [42].

The two types of engines are characterized by the data reported in Table 1.

The characterization about the engine fuel consumption is based on data in Figure 7 where the trend of the engine efficiency (η) vs. %MCR is reported. It applies for both engine types because they differ only in the number of cylinders. All data have been obtained from [42]. The constraints concerning the behavior of this component, represented by Eq. (10), have been approximated by a polynomial curve of the 3rd order. The adopted modularity allows ICEs to always operate in a range from 75 to 98 of %MCR (regardless of the season and the different phase of the cruise). It follows that, thanks to the flattened shape of efficiency-%MCR curve, ICEs work with a mean efficiency of about 45.1 %, i.e. only 2% less compared to the peak value of 47.8 %, reached at 87 of %MCR.

Table 1. Wärtsilä #46C' technical data [42].

Nominal speed	514	[rpm]
Bore	460	[mm]
Stroke	580	[mm]
Maximum Continuous Output	1050	[kW/cyl]

4.2 Gas turbines

A survey was carried out in order to find out the most suitable gas turbines for this application: Siemens SGT-300 and Siemens SGT-400 were selected. The main technical data in design mode have been taken from [43, 44] and are reported in the first two columns of Table 2.

The off-design data not being available in the above-cited literature, a virtual model of both GTs has been developed by the commercial software, THERMOFLEX[®] provided by Thermoflow Inc. Fig. 8 shows the computed efficiency trends as a function of %MCR, for the selected GTs.

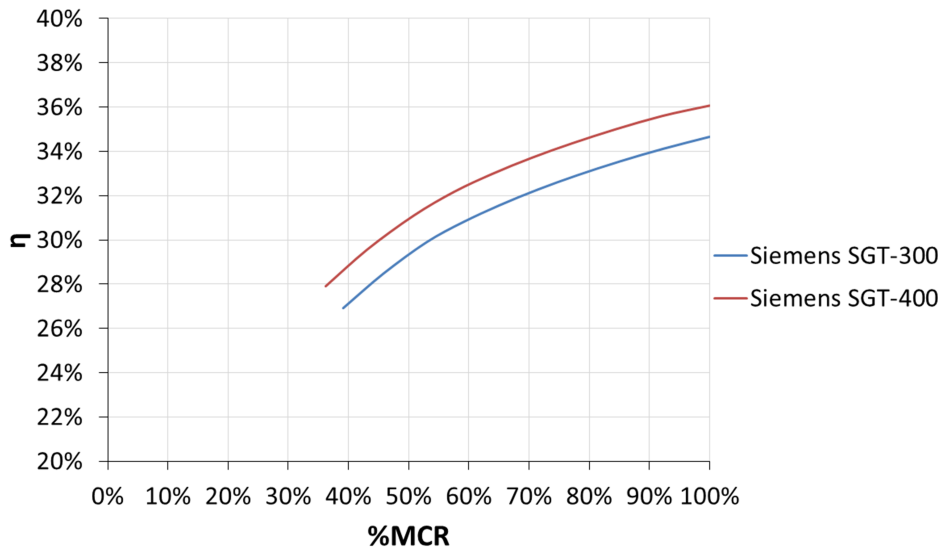


Fig. 8. Siemens GT-400 efficiency Vs. %MCR of the selected GTs.

Table 2. Performance data of real GTs [43, 44] and Virtual ones.

Parameters	Siemens SGT-300	Siemens SGT-400	Type A	Type B	
Nominal Power	8.7	13.5	8.3	10.6	[MW]
Air mass flow	29.99	38.90	28.6	30.5	[kg/s]
Exhaust gas flows	26.98	39.28	26.1	31	[kg/s]
TOT	497.7	545.3	497.7	545.3	[°C]
TIT	1100	1290	1100	1290	[°C]
RPM	14010	14100	14010	14100	[rpm]
η (@100 %MCR)	34.65	36.07	34.65	36.07	[-]
η (@ 90 %MCR)	33.94	35.44	33.94	35.44	[-]
η (@ 80 %MCR)	33.09	34.62	33.09	34.62	[-]

The virtual model has also been used in order to define two more scaled-down GTs, namely Type A and B, whose data are reported in the last two columns of Table 2. The operation has been necessary in view of the slightly higher nominal power output that is found for the two selected Siemens GTs compared to that of the ICEs installed on the reference ship. Indeed, in view of the electric loads reported in Fig. 5 and as a consequence of the efficiency trend reported in Fig. 8(b), such higher nominal power would require the GT to be operated too far from its optimal conditions, hence increasing even more the efficiency gap compared to ICEs.

The size coefficient of the scaled-down GTs has been determined so that they can be mostly operated with a load above 95%. In more detail, SGT-300's power output has been decreased by 3% and SGT-400 by 21%. In order to have the same power installed on board, the employment of one more gas turbine, having a power output equal to 5 MW, has been also considered just for safety purposes.

4.3 Exhaust Gas Boilers

The technical data for the EGB employed on the reference ship was supplied by [40]. The amount of steam produced depends on the engine type and load: nominal steam production is referred to ICE nominal load, namely 80% MCR, and Eq. (10) can be approximated by means of a 3rd order polynomial.

These data are relative to ICEs and therefore, if solutions based on GTs have to be considered, to use the same EGBs would be wrong due to the different enthalpy flows of the exhaust gas. Therefore, the design of suitable EGB for GT application is necessary for each Type of GT.

Hence, not only an operational optimization but also a design optimization has been carried out for all the GT configurations. The target is to find the EGBs that provides the best compromise between weight and volume and ship energy efficiency (or percentage of cogeneration).

Weight and volume of the EGBs has been calculated starting from the data of the systems used for ICE application and by making a proportion with the thermal power exchanged by the two configurations, i.e. ICE and GT.

To take into account a wide spread of EGB size, it has been chosen to consider 10 possible EGBs that have different delta T pinch points (Table 3). Two extreme EGBs have been identified, characterized by a minimum delta T pinch point of 34°C and a maximum of 304°C. These values are justified by the fact that 34°C is equal to that of ICEs and 304°C is the delta T pinch point that is necessary to produce with the GT EGB the same design value of steam flow produced in the ICE case.

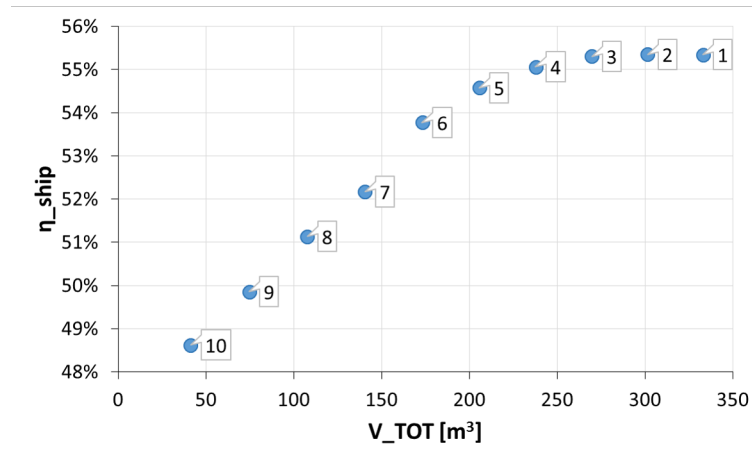


Fig. 9. Annual average global ship efficiency for the 10 selected EGB Vs. the total volume occupied.

Determination of EGB data in design mode has been conducted with THERMOFLEX[®]. Once design mode was provided, off-design conditions have been simulated too by varying GT %MCR.

After this procedure, a function expressing thermal power recoverable vs. GT load has been implemented in the optimization procedure of the ship operation profile to compute the annual average global ship efficiency for every EGB considered. In particular, the model sets that just the steam flow useful to cover the thermal loads is produced in the EGB. This means that once the thermal loads are satisfied, i.e. the useful steam production is reached, the waste heat content of the exhaust gas flows is not exploited any more. As a consequence, exhaust gas could further be exploited to cover other thermal loads, i.e. that linked to fresh water production or to satisfy the ship chilling load if eventually trigeneration systems were taken into consideration.

Table 3. Delta T Pinch Points values, at design conditions for the 10 EGB considered..

#EGB	Delta T [°C]
1	34
2	64
3	94
4	124
5	154
6	184
7	214
8	244
9	274
10	304

The graph in Fig. 9 reports the annual average global ship efficiency for the 10 selected EGB vs. the total volume occupied. It can be noted that the curve has a not very sharp maximum for a volume of about 300 m³. The assumed selection criteria considers the configuration with minimum volume, allowing at the same time an efficiency reduction smaller than 0.5% compared to the maximum. Then, the analysis of the plot suggests that the best EGB option is the number 4: since it allows having fairly good ship efficiency (55%) with a reasonable volume occupied (238 m³). Furthermore, it can be noted that after a certain point, the efficiency does not increase any more even if further water vapor could be produced: to increase the EGB size to exploit all the waste heat content in the exhaust gas flow is not fruitful in this specific application. Indeed, the smallest EGB (n°10) provides the lowest amount of energy recovered but the highest exhaust gas temperature from the EGB. On the other hand, the biggest EGB (n°1) provides the largest amount of energy recovered but the lowest exhaust gas temperature from the EGB, as can be noted in Fig. 10. Therefore, a compromise has to be reached and hence EGB n°4 was selected, which can recover $2,9 \cdot 10^6$ MJ and has an exhaust gas temperature equal to 360°C. Both values have to be understood as mean values with three seasons considered.

4.4 Exhaust gas after-treatment devices

Every internal combustion engine has its own SCR reactor that consists of an inlet and an outlet duct, catalyst layers, a steel structure for supporting the catalyst layers and a soot-blowing unit. According to [45], SCR efficiency is considered to be equal to 85% regardless of the engine load (i.e. exhaust gas temperatures, mass flow, NO_x content, ...).

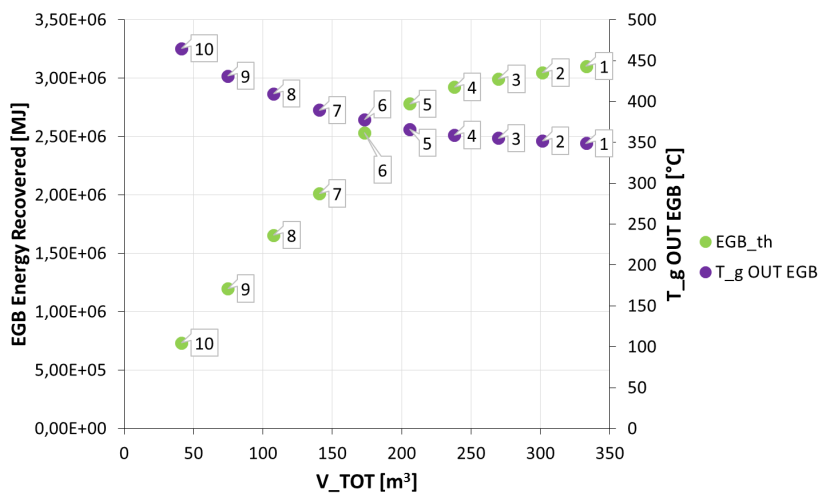


Fig. 10. Annual average energy recovered by EGB use and exhaust gas Temperature ($T_g OUT EGB$) vs. total volume occupied for every #EGB.

In the reference cruise ship, SCRs are considered to be placed immediately after the engines and have an electric overall power demand of 50 kW. This choice has been made in order to always have an exhaust gas temperature high enough to avoid the risk of hydrocarbon condensation and ammonium sulphate formation, and, at the same time, to

achieve/maintain a good efficiency despite the possible catalyst deterioration caused by high temperatures and the passage of very dirty exhaust gases.

In this work, two kinds of scrubbers were studied in order to evaluate which one could be the most suitable for an on-board application, namely dry scrubbers and wet scrubbers.

Considering the storage issues concerned with the use of dry scrubbers, wet ones have been chosen, in particular closed loop wet scrubbers that are independent of seawater quality. Closed Loop Scrubbers have an efficiency of 97% [46] and require an overall extra electrical power of 34 kW.

Low SO_x emissions could also be achieved without Scrubbers, but switching to a fuel with a lower sulphur content. It has to be underlined that, in this study, only ICE exhaust gas flows are treated with these devices, meanwhile exhaust gas flows deriving from OFB are released into the atmosphere without being cleaned.

4.5 Emission modeling

Regarding pollutant emissions, the choice made was to follow the method suggested by Haglind [27], who reported a list of pollutant emissions factors in order to overcome the lack of pollutant emissions technical data provided directly by the engine constructors. Therefore, pollutant emissions calculations are made once the optimization procedure has been completed. In particular, emission factors depend on the fuel quality [47], the combustion mode, and they are expressed as g_{pollutants}/kg_{fuel}. Pollutant emissions here considered can be divided into two groups: {PM, SO_x and HC} and {NO_x and CO}.

This distinction is the result of each group dependency on fuel quality rather than combustion mode: the first group is linked to the fuel quality and the second one to the combustion mode. As far as the SO_x emission factor is concerned, it depends only on the fuel sulphur content. Indeed, considering all SO_x as SO₂, the emission factor has been calculated as reported in Eq. (11):

$$EF_{SO_x} = 2 \times \%S_{fuel} \quad [\text{g}_{\text{pollutants}}/\text{kg}_{\text{fuel}}] \quad (11)$$

From what that can be found in [48], the mean percentage of sulphur content is 2.7% and 0.1% for HFO and MGO respectively. Consequently, emission factors calculated by means of Eq. (11) are 54 g_{SO_x}/kg_{fuel} for HFO and 2 g_{SO_x}/kg_{fuel} for MGO. Emission factors for all the pollutants considered are reported in Tab. 4, depending on fuel quality (HFO and MGO) and combustion mode (OFB, GT and ICE).

Table 4. Pollutants emission factors [g_{pollutants}/kg_{fuel}] depending on the fuel quality and its utilization.

	ICEs_HFO	GTs_MGO	OFBs	
			HFO	MGO
CO	7.4	2.2 (=10 ppm) [28, 29]	0.14	0.14
PM	7.6	1.1	7.6	1.1
SO_x	54	2	54	2
NO_x	87	8 (=15ppm) [28, 29]	28.6	28.6
HC	2.7	0.05	2.7	0.05

Therefore, once having the total amount of fuel burned, the general Eq. (12) is used for every type of pollutants:

$$PE_h = EF_h \times Fuel \times 1000 \quad [\text{g}] \quad (12)$$

where PE_h is the h-th pollutant emissions, EF_h is the h-th pollutant emission factors reported in Table 4 and $Fuel$ is the total amount of fuel burned in ICEs, GTs and OFBs.

For the ICE_{eco} case, the abatement efficiency of SCR and scrubber have to be taken into account, resulting in the following two new equations:

$$PE_{NO_x} = EF_{ICE_{NO_x}} \times Fuel_{ICE} \times \eta_{SCR} \quad [\text{g}] \quad (13)$$

$$PE_{SO_x} = EF_{ICE_{SO_x}} \times Fuel_{ICE} \times \eta_{scrubber} \quad [\text{g}] \quad (14)$$

where $EF_{ICE,NOx}$ is the NO_x emission factor specific for the ICE, $EF_{ICE,SOx}$ is the emission factor for HFO use, η_{SCR} is the SCR abatement efficiency equal to 85%, and $\eta_{scrubber}$ is the scrubber abatement efficiency equal to 97%.

5. Results

In this paragraph, results obtained by the optimization procedure are presented in terms of global ship energy efficiency and amount of pollutant emissions during the whole cruise. The different weight and volume occupied by the PMs and their auxiliary devices are also computed in the optimization procedure.

Table 5. Case summary of engines configurations and global ship energetic efficiency ($\eta_{ship,global}$) for the different seasons.

	Engine type	Fuel	SCR	Scrubber	$\eta_{ship,global}$ W	$\eta_{ship,global}$ S	$\eta_{ship,global}$ A
ICE	2 x W12V46C 2 x W8L46C	HFO	No	No	67.1%	64.7%	63.8%
ICE_eco	2 x W12V46C 2 x W8L46C	HFO	Yes	Yes	66.7%	64.5%	63.5%
GT	2 x Type A 8.3MW 2 x Type B 10.6MW	MGO	No	No	59.7%	53.8%	52.0%

Table 5 summarizes the main characteristics of the three engine configurations analyzed and reports the results of the global ship energy efficiency for each configuration, for the three kind of season (winter – W, summer – S and autumn + spring – A). The ICE case always obtains the best results. The supplementary energy demand of the auxiliaries of SCR and scrubber systems installed in the ICE_Eco case causes an efficiency drop of about 1%. Both ICE and ICE_eco cases are only marginally affected by the seasonal changes. On the contrary, GT configuration is noticeably more sensitive to climate variability resulting to strong variations of the efficiency gap, as opposed to the ICE case, ranging from –6% for winter up to –13% for autumn.

The higher GT cogeneration capability reduces the initial gap with ICE caused by the lower electrical efficiency, especially for winter-harbor condition, when the thermal loads are the highest. Nevertheless, the available heat for GT case often exceeds the thermal demand (34% as average), hence causing a remarkable energy waste that, at the end, results in the observed negative gap about $\eta_{ship,global}$. The same observation explains the strong dependence of GT efficiency on seasonal changes, the thermal loads being closely linked to the climate conditions.

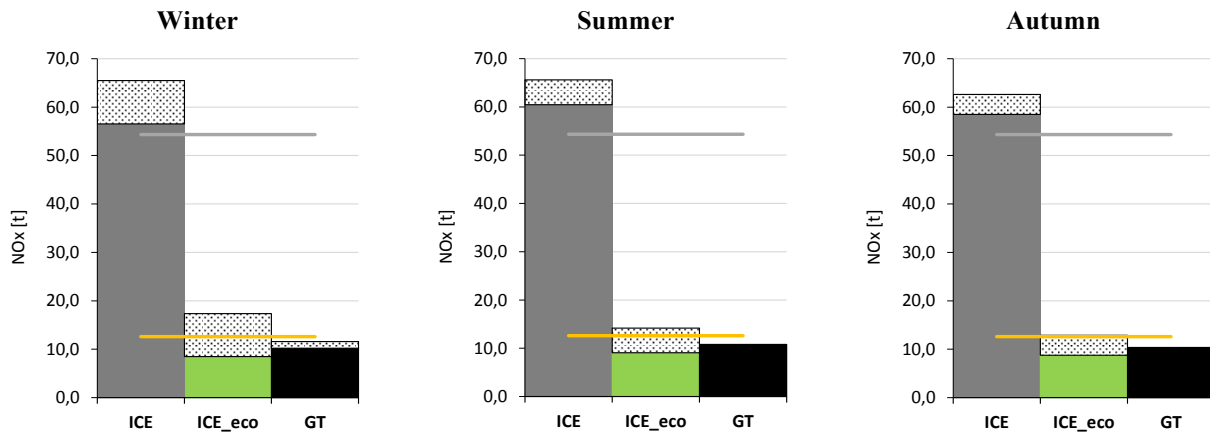


Fig. 11. Overall cruise NO_x emissions for every season and engines' configuration compared with Tier II (bold grey line) and Tier III (bold yellow line) emissions, as well as OFBs' emissions (dotted area).

Figure 11 provides the overall NO_x emissions produced during the cruise for the analyzed configurations, and provides also a comparison between the three seasonal conditions. Data have been computed relying on specific factors provided by the producers: in particular 12 g NO_x /kWh for ICEs [42] and 15ppmv of NO_x at 15% O_2 for GTs [43, 44].

An indication of MARPOL requirements is provided by reporting the threshold values of both Tier II (bold grey line), and Tier III (bold yellow line). In particular, the threshold specific factors for ICEs are directly computed on the basis of the actual engine speed (514 rpm), conversely for GTs a lack in the regulations has been highlighted. Indeed, IMO

documentation regards only the use of ICEs, therefore, in order to compute a reference limit for the GTs, a conservative choice was made by picking the lowest values reported in the regulations.

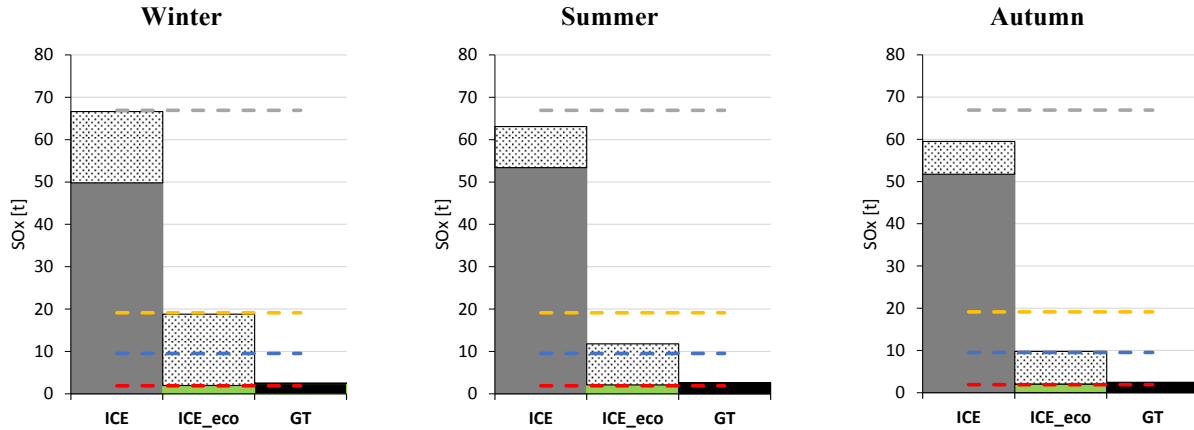


Fig. 12. Overall cruise SO_x emissions for every season and engines configuration compared with different fuel Sulphur content thresholds (dashed lines) as well as OFB emissions (dotted area).

In order to make a fair comparison, even if not specifically considered by MARPOL, in the present study also NO_x emissions coming from OFB have been taken into account (dotted area in Fig. 11).

The results obtained for the ICE case show that the traditional configuration is far above the limits imposed by Tier III (about +360%), and exceeds also the ones of Tier II, even if by a rather small amount. If the latter issue could be easily overcome thanks to the improvements of the combustion systems adopted on modern ICEs, at present, Tier III limits can be reached only by the adoption of SCR systems as done in the ICE_eco case. Conversely, and as expected, NO_x emissions by GTs are noticeably reduced, even without SCR devices, and turned out to be in line with the stricter thresholds limits here considered. Moreover, nowadays even lower NO_x emissions factors (about 9 ppmv [43, 44]) can be easily obtained, thanks to new Dry Low NO_x combustion systems.

By considering OFB emissions as well, the negative gap of the ICE case widens considerably, and also for the ICE_eco case the limits are exceeded; on the contrary, GT configuration is not affected, the use of OFB being rather marginal.

The results concerning SO_x emissions are reported in Figure 12. Dashed lines indicate MARPOL limits computed on the basis of the different thresholds imposed on the fuel sulphur content, in particular: grey, yellow, blue and red stand for 3.5, 1, 0.5 and 0.1 %S, respectively. Moreover, OFBs SO_x emissions are considered too (dotted area in Figure 12).

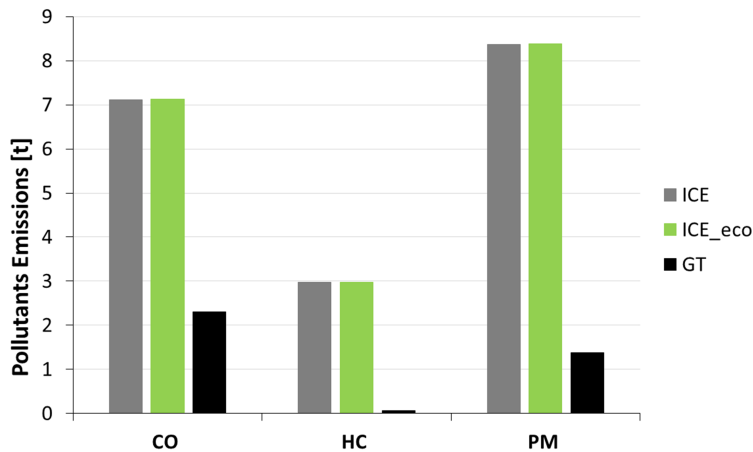


Fig. 13. Cruise ship overall-CO, HC, and PM emissions in autumn season.

By analyzing Figure 12 it can be inferred that in order to travel through SECA seas, ICE configuration ought to reduce SO_x emissions by at least an average of 63%. The said reduction is definitely secured by the ICE_eco solution where the scrubber abatement efficiency allows to respect even the stricter future limitations. Thanks to the use of MGO, SO_x emission in the GT case are comparable to the ones of the ICE_eco, but they are a little over the “SO_x 0.1” threshold level (i.e. the SO_x emissions resulting from ICE burning fuel with 0.1% sulphur content, such as MGO). This issue is a direct consequence of the higher GT fuel consumption than ICEs. Finally, regarding SO_x, if the contribution of the OFB

is also considered, the difference between GT and ICE_eco cases widens considerably, with the latter exceeding also SO_x 0.5 limit.

Overall emissions in term of CO, PM and HC for the three configurations are reported in Figure 13 for the autumn season. Since the abatement devices are ineffectual against CO, HC and PM emissions, ICE and ICE_eco have the same behavior regarding these pollutants. In particular the latter registers a little more (+0.44% CO; +2.80% HC and PM) pollutants emissions than the former because of the higher fuel consumption previously commented. Thanks to a different kind of combustion mode, GTs are the cleanest from this point of view. GTs have -97% CO and -83% of HC and PM than ICEs.

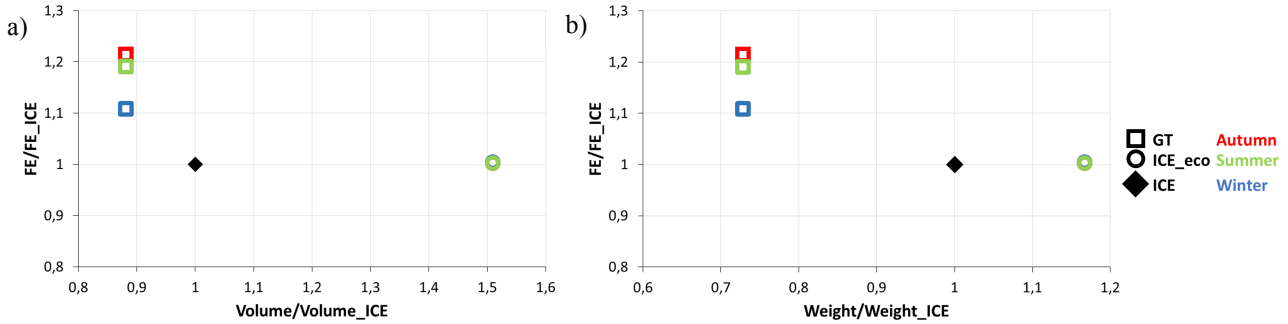


Fig. 14. FE vs. Volume (a) and Weight (b) normalized with the ICE case.

The last comparison consists in quantifying the gap existing between all the configurations in terms of space and weight versus the fuel consumption. The reference ship shows average fuel consumption during a cruise of 1150 t of HFO.

Given the different LHV of MGO and HFO, the fuel consumption is provided as Fuel Energy (FE) content, which is equal to $E_{fuel,global}$ reported in Eq. (1), instead of tons of fuel, and it has been computed considering the fuel burned by both PMs and OFBs. The data about weight and space are computed by considering the contribution of PMs, EGBs, compressor chillers, and pollutant abatement devices (when necessary), and are derived by the technical specifications of the different systems.

In order to ease the analysis, the data reported in Figure 14 have been normalized for the values of the ICE case.

The expected space and weight saving consequent to the use of GTs is quite clear, with a reduction of 11% and 27% of volume and weight respectively, compared to the current ICE case. These percentages correspond to free 125m³ and to lighten the reference cruise ship of 232 ton.

Concerning the ICE_eco case, the use of abatement device involves an increase of about 50% of the volume occupied on board (+440m³) and an increase of the ship weight of +17% (+144 ton) keeping ICE case as base model.

The advantages of the GT case are even more striking if the ICE_eco case is considered. In particular, the use of pollutant abatement devices of the ICE_eco solution increases the ratio up to more than 150% both for the volume and the weight, namely the difference in volume occupied on board and in weight is equal to 666 m³ and 376 tons respectively.

Finally, a comparison of cruise averaged values of the global ship's energetic efficiency computed for the three cases and for different seasons is reported in Figure 15.

The highest efficiency is always attained by ICE case. ICE_eco is negatively affected by the supplementary energy demand of the auxiliaries of SCR and scrubber systems that cause a ship efficiency drop of about 1%. Both ICE and ICE_eco cases are only marginally affected by the seasonal changes. On the contrary, GT configuration is rather more sensitive to climate variability. The resulting variations of the efficiency gap with respect to ICE case, range from -6% during winter up to -13% during autumn.

The lower GT configuration ship efficiency can be explained if a detailed analysis is carried out, considering the different cruise phases harbor and navigation, regarding as negligible the maneuvering phase because it has a very little impact on the all cruise. Figure 16 shows, as an example, the ship's energy efficiency during autumn season. It can be noted that the efficiency gap between GT and ICEs is erased when harbor phase only is taken into account. On the other hand, GT configuration is 10 points percentage less efficient than ICEs configurations if the navigation phase is considered.

Subdividing the ship annual average efficiency into propulsion efficiency and cogenerable fraction of thermal load, it can be understood the reason why GT configuration has the same energy efficiency in harbor but not during the navigation phase. Indeed, GT configuration can reach the same ship's energy efficiency thanks to its high capability of

cogeneration that allows reducing the gap existing in terms of propulsion efficiency when the ship is in harbor. This situation does not happen during navigation, where the cogenerable part of the thermal load is not enough to reduce the propulsion efficiency gap, which remains more or less constant. It can be easily inferred that an extensive thermal load cogeneration is a key factor in determining the ship efficiency.

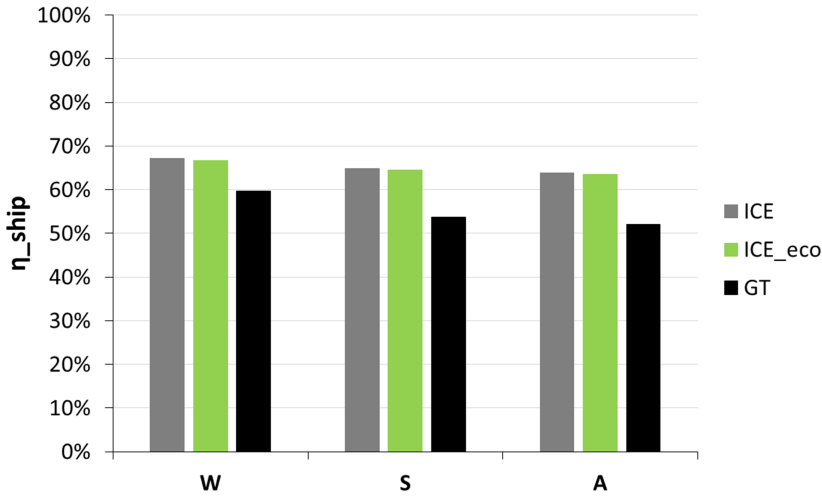


Fig. 15. Global ship efficiency for the 3 engine configurations, in different seasons.

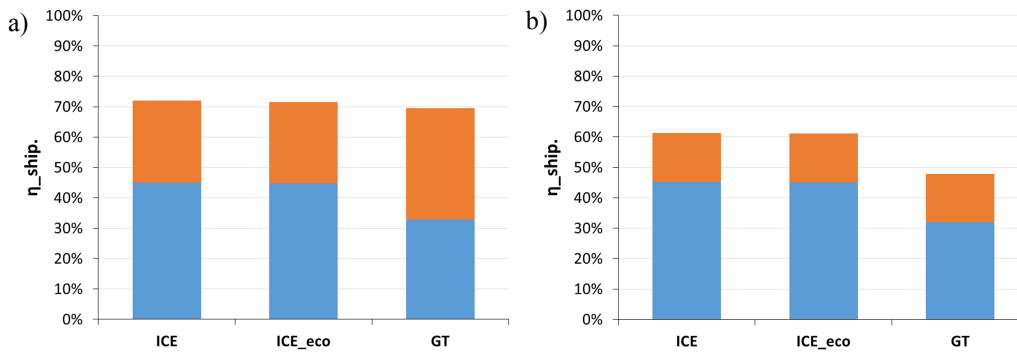


Fig. 16. Global ship efficiency for the 3 engine configurations, in autumn season, for harbor (a) and navigation phase (b). In orange the cogeneration fraction.

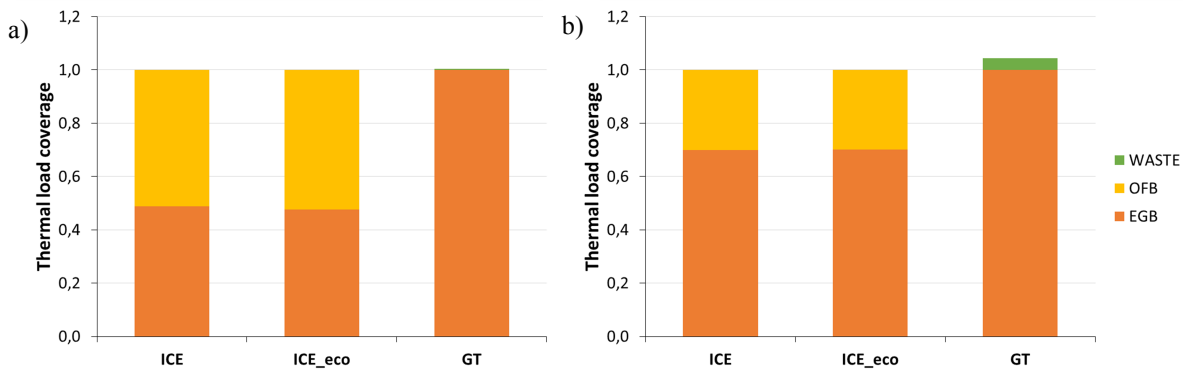


Fig. 17. Ship thermal load coverage in autumn season, for harbor (a) and navigation phase (b).

Results of a more detailed analysis regarding how thermal loads are covered are shown in Figure 17. These graphs show how the thermal energy is obtained through cogeneration (orange bar) or employing OFB (yellow bar). Finally, the green bar represents the waste heat flux, if any.

This analysis shows that, for maximizing ship efficiency, it is essential to cover the most part of thermal load by using the exhaust gas flows, instead of the OFB, reducing to the maximum extent the amount of waste heat. This condition is favorable to GT, in particular in the harbor phase, where the high possibility of cogeneration allows the reduction of the

existing gap in propulsion efficiency. During navigation the electric load is much higher and a part of the recoverable heat has to be dissipated. Therefore the benefit obtained by the cogeneration is not enough to compensate the efficiency gap.

6. Conclusions

In order to be compliant with new IMO regulations about pollutant emissions, the conventional system based on ICE (ICE case) has to be modified, either by installing De-SO_x and De-NO_x abatement devices on the original propulsion system (ICE_eco case), based on HFO fueled ICEs, or by replacing it with MGO fueled GTs (GT case). The objective of the present work was to quantify the differences in terms of weight, volume, and fuel consumption of the different designs of the on-board energy system for application on a cruise ship.

This study considers the actual phases of a tourist cruise between Barcelona and Venice, not focusing on the design condition only of the on-board energy system, and may be of interest for ship owners since there are only few studies of this kind available in literature.

To achieve the target, an optimization procedure has been used with the goal of minimizing the total amount of fuel burnt by the prime movers. Because of the presence of both discrete and integer variables as well as of non-linear equations linked to the operating conditions of the major components, a MINLP problem has emerged, which needed to be solved by the adopted evolutionary algorithm. Successively, pollutant emissions were calculated and finally the different engines configurations have been characterized in terms of weight and volume required by the adopted energy conversion systems.

The analysis of the results shows that to employ GTs as prime movers leads to both environmental, weight, and volume benefits. Moreover, thanks to the relevant amount of heat recovered, Oil Fuel Burner use is marginal with a further positive effect on the overall ship pollutant emissions, conversely to what has been observed for solutions based on ICEs where MARPOL threshold limits would be exceeded if OFB pollutant emissions were considered.

On the other hand, the lower electric efficiency of GTs causes a drop in the whole ship energy efficiency, whose amount results to be also sensitive to seasonal variations. The additional fuel consumption, compared to ICE case, ranges between +10 to +20%, in the different seasons, with an expected year fuel consumption increase of about 18%. However, by considering that the volume reduction can reach 40% of the ICE_eco case, it results that the identification of the most convenient solution depends on the economic value given to the on-board volume availability.

It is worth noting that the heat recovered in the GT case allows this solution to reach the same ship efficiency of the ICE case in the harbor phase. In the navigation phase the load of the engine is higher and the amount of recoverable heat from the exhaust flow in the GT case (not in the ICE cases) exceeds the total thermal demand and has to be partially dissipated. This consideration suggests that the efficiency gap between the considered PMs should be reduced in the navigation phase also if the exceeding heat were used to activate an absorption chiller, with a positive effect on the non-propulsive power demand. In this case, the on-board energy system should be converted into a trigeneration system.

The information in this study may help the operators of the marine sector and decision makers in evaluating and designing future solutions for sustainable shipping and emission regulations.

Acknowledgements

The authors are grateful to Fincantieri S.p.A. for having allowed accessing the data necessary to carry out this research.

References

- [1] International Maritime Organization, International Shipping Facts and Figures – Information Resources on Trade, Safety, Security, Environment, 2012.
- [2] Maragkogianni A, Papaefthimiou S, Evaluating the social cost of cruise ships air emissions in major ports of Greece, Transp. Res. Part D Transp. Environ. 2015; 36; 10–17.
- [3] Anderson K, Bows A, Executing a Scharnow turn: reconciling shipping emissions with international commitments on climate change, Carbon Management 2012; 3 (6); 615-28.
- [4] International Maritime Organization, MARPOL 73/78. Annex VI, 1997.
- [5] Buhaug K, Corbett Ø, Endresen J J, Eyring Ø, Faber V, Hanayama J, Lee S, Lee D S, Lindstad D, Markowska H, Mjelde A Z, Nelissen A, Nilsen D, Pålsson J, Winebrake C, Wu J J, Yoshida W, Second IMO GHG Study 2009.

- [6] International Maritime Organization, RESOLUTION MEPC. 2008; 176 (58).
- [7] Lloyd's Register, LNG-fuelled deep sea shipping: The outlook for LNG bunker and LNG-fuelled newbuild demand up to 2025, August 2012;
- [8] Burel F, Taccani R, Zuliani N, Improving sustainability of maritime transport through utilization of Liquefied Natural Gas (LNG) for propulsion, *Energy* 2013; 49; 412-20.
- [9] Livanos G A, Theotokatos G, Pagonis D N, Techno-economic investigation of alternative propulsion plants for Ferries and RoRo ships , *Energy Conversion and Management* 2014; 79; 640-51.
- [10] Banawan AA, El Gohary MM, Sadek IS, Environmental and economical benefits of changing from marine diesel oil to natural-gas fuel for short-voyage high-power passenger ships, *Proceedings of the Institution of Mechanical Engineers Part M Journal of Engineering for the Maritime Environment* 2010; 224(2); 103-13.
- [11] Helfre J, Boot P A C, Emission Reduction in the Shipping Industry : Regulations , Exposure and Solutions, *Exposure and Solutions*, 2013.
- [12] Raptotasios S I, Sakellariadis N F, Papagiannakis R G, Hountalas D T, Application of a multi-zone combustion model to investigate the NOx reduction potential of two-stroke marine diesel engines using EGR, *Applied Energy* 2015; 157; 814–23.
- [13] Lamas MI, Rodriguez CG, Emissions from Marine Engines and NOx Reduction Methods, *J. of Maritime Research* 2012; 1 (9); 77-82.
- [14] Azzara AA, Rutherford D, Wang H, Feasibility of IMO Annex VI Tier III implementation using Selective Catalytic Reduction, *International Council on Clean Transportation*, 2014.
- [15] Petersen PD, MAN Diesel & Turbo Delivers World's First IMO-Certified Two-Stroke Engine with Tier III NOx Control, Exhaust Gas Recirculation Systems, *MAN Global Corporate Website*, 2016.
- [16] Imperato M, Kaario O, Sarjovaara T, Larimi M, Wik C, Zero NOx emission in large-bore medium speed engines with exhaust gas recirculation, in: *Proceeding CIMAC Congress 2016*, Helsinki, Paper N° 58.
- [17] Yang F, Dong X, Zhang H, Wang Z, Yang K, Zhang J, Wang E, Liu H, Zhao G, Performance analysis of waste heat recovery with a dual loop organic Rankine cycle (ORC) system for diesel engine under various operating conditions, *Energy Conversion and Management* 2014; 80; 243–55.
- [18] Bonafin J, Pinamonti P, Reini M, Tremuli P, Performance improving of an internal combustion engine for ship propulsion with a bottom ORC. In: *Proceedings of ECOS 2010*.
- [19] Mondejar ME, Ahlgren F, Thern M, Genrup M, Quasi-steady state simulation of an organic Rankine cycle for waste heat recovery in a passenger vessel, *Applied Energy* 2017; 185; 1324–1335.
- [20] Min-Hsiung Yang, Rong-Hua Yeh, Thermodynamic and economic performances optimization of an organic Rankine cycle system utilizing exhaust gas of a large marine diesel engine, *Applied Energy* 2015; 149; 1–12.
- [21] Rech S, Zandarin S, Lazzaretto A, Frangopoulos CA, Design and off-design models of single and two-stage ORC systems on board a LNG carrier for the search of the optimal performance and control strategy. *Applied Energy* 2017; 204; 221–41.
- [22] Tien W K, Yeh R H, Hong J M, Theoretical analysis of cogeneration system for ships, *Energy Conversion and Management* 2007; 48; 1965–74.
- [23] Dzida M, Possible Efficiency Increasing of Ship Propulsion and Marine Power Plant with the System Combined of Marine Diesel Engine, Gas Turbine and Steam Turbine, *Advances in Gas Turbine Technology* 2011; November; 45-68.
- [24] Haglind F, A review on the use of gas and steam turbine combined cycles as prime movers for large ships. Part I: Background and design, *Energy Conversion and Management* 2008; 49; 3458–67.
- [25] Bosich D, Vincenzutti A, Pelaschiar R, Menis R, Sulligoi G, Towards the future: the MVDC large ship research program, 2015, http://www.aeit.it/man/CA2015/atti/sessione_C2/C2_01.pdf.
- [26] Sannemann B N, Pioneering gas turbine-electric system in cruise ships: a performance update, *Marine Technology and SNAME News* 2004; 41 (4); 161-66.
- [27] Haglind F, A review on the use of gas and steam turbine combined cycles as prime movers for large ships. Part II: Previous work and implications, *Energy Conversion and Management* 2008; 49; 3468–75.
- [28] Ren H, Zhou W, Nakagami K, Gao W, Wu Q. Multi-objective optimization for the operation of distributed energy systems considering economic and environmental aspects. *Applied Energy* 2010; 87 (12):3642-51.
- [29] Carvalho M, Lozano MA, Serra LM. Multicriteria synthesis of trigeneration systems considering economic and environmental aspects. *Applied Energy* 2012;91(1); 245-54.
- [30] Dai R, Mesbahi M, Optimal power generation and load management for off-grid hybrid power systems with renewable sources via mixed-integer programming. *Energy Conversion and Management* 2013; 73; 234-44.

- [31] Casisi M, Pinamonti P, Reini M. Optimal lay-out and operation of CHP distributed energy systems. *Energy* 2009;34 (12); 2175-83.
- [32] Buoro D, Casisi M, De Nardi A, Pinamonti P, Reini M. Multicriteria optimization of a distributed energy supply system for an industrial area. *Energy* 2013; 58; 128-37.
- [33] Lozano MA, Ramos JC, Serra LM. Cost optimization of the design of CHCP (combined heat, cooling and power) systems under legal constraints. *Energy* 2010; 35; 794-805.
- [34] Bojic M, Stojanovic B. MILP optimization of a CHP energy system. *Energy Conversion and Management* 1998; 39 (7); 637-42.
- [35] Yokoyama R, Ito K. Operational strategy of a cogeneration system under a complex utility rate structure. *Journal of energy resources technology* 1996; 118 (4); 256-62.
- [36] Tostevin G M, Nealy J C, Computer synthesis for the design of marine power plants, *J. Mar. Res. B* 2003.
- [37] Kougioufas A, Marine energy system optimization with reliability and availability considerations, Diploma Thesis 2005, National Technical University of Athens, Athens, Greece.
- [38] Armellini A, Daniotti S, Pinamonti P, Gas Turbines for Power Generation on Board of Cruise Ships: A Possible Solution to Meet the New IMO Regulations?. *Energy Procedia* 2015; 81; 540–47.
- [39] Fincantieri S.p.A., Electric Loads. 2012.
- [40] Fincantieri S.p.A., Thermal Loads. 2012.
- [41] Dimopoulos G G, Kougioufas A V, Frangopoulos C A, Synthesis, design and operation optimization of a marine energy system. *Energy* 2008; 33 (2); 180–88.
- [42] Wärtsilä, Project Guide. 2007.
- [43] Siemens, SGT-300 Technical Data. 2012; 0–3.
- [44] Siemens, SGT-400 Technical Data. 2013; 31.
- [45] Fincantieri S.p.A., Private communications. 2014.
- [46] U.S.A. Environmental Protection Agency, Exhaust Gas Scrubber Washwater Effluent, Washington (USA), 2011.
- [47] Mueller L et al., Characteristics and temporal evolution of particulate emissions from a ship diesel engine, *Applied Energy* 2015; 155; 204–17.
- [48] Endresen Ø, Sørgård E, Sundet J K, Dalsøren JS B, Isaksen I S A, Berglen T F, Gravir G, Emission from international sea transportation and environmental impact, *Journal of Geophysical Research* 2003; 108 (D17).